

## 6 An Assessment of the Precision and Confidence of Aquatic Eddy Correlation Measurements

DAPHNE DONIS,<sup>a</sup> MORITZ HOLTAPPELS,<sup>b</sup> CHRISTIAN NOSS,<sup>c</sup> CECILE CATHALOT,<sup>d,e</sup> KASPER HANCKE,<sup>f</sup>  
 PIERRE POLSENAERE,<sup>g,h</sup> FRANK WENZHÖFER,<sup>a</sup> ANDREAS LORKE,<sup>c</sup> FILIP J. R. MEYSMAN,<sup>i</sup>  
 RONNIE N. GLUD,<sup>j</sup> AND DANIEL F. MCGINNIS<sup>k,l</sup>

<sup>a</sup> HGF MPG Research Group for Deep-Sea Ecology and Technology, Alfred Wegener Institute Helmholtz Centre for Polar and Marine Research, Bremerhaven, and Max Planck Institute for Marine Microbiology, Bremen, Germany

<sup>b</sup> Department of Biogeochemistry, Max Planck Institute for Marine Microbiology, Bremen, Germany

<sup>c</sup> Institute for Environmental Sciences, University of Koblenz-Landau, Landau, Germany

<sup>d</sup> Royal Netherland Institute for Sea Research (NIOZ), Yerseke, Netherlands

<sup>f</sup> Nordic Center for Earth Evolution, Department of Biology, University of Southern Denmark, Odense, Denmark, and Greenland Climate Research Centre, Greenland Institute of Natural Resources, Nuuk, Greenland

<sup>g</sup> Department of Analytical, Environmental and Geo-Chemistry, Vrije Universiteit Brussel, Brussels, Belgium

<sup>i</sup> Royal Netherland Institute for Sea Research (NIOZ), Yerseke, Netherlands, and Department of Analytical, Environmental and Geo-Chemistry, Vrije Universiteit Brussel, Brussels, Belgium

<sup>j</sup> Nordic Center for Earth Evolution, Department of Biology, University of Southern Denmark, Odense, Denmark, and Greenland Climate Research Centre, Greenland Institute of Natural Resources, Nuuk, Greenland, and Arctic Research Centre, University of Aarhus, Aarhus, Denmark, and Scottish Marine Institute, Scottish Association for Marine Science, Oban, United Kingdom

<sup>k</sup> Nordic Center for Earth Evolution, Department of Biology, University of Southern Denmark, Odense, Denmark, and Department of Experimental Limnology, Leibniz-Institute of Freshwater Ecology and Inland Fisheries, Berlin, Germany

(Manuscript received 15 April 2014, in final form 16 September 2014)

### ABSTRACT

The quantification of benthic fluxes with the aquatic eddy correlation (EC) technique is based on simultaneous measurement of the current velocity and a targeted bottom water parameter (e.g., O<sub>2</sub>, temperature). High-frequency measurements (64 Hz) are performed at a single point above the seafloor using an acoustic Doppler velocimeter (ADV) and a fast-responding sensor. The advantages of aquatic EC technique are that 1) it is noninvasive, 2) it integrates fluxes over a large area, and 3) it accounts for in situ hydrodynamics. The aquatic EC has gained acceptance as a powerful technique; however, an accurate assessment of the errors introduced by the spatial alignment of velocity and water constituent measurements and by their different response times is still needed.

Here, this paper discusses uncertainties and biases in the data treatment based on oxygen EC flux measurements in a large-scale flume facility with well-constrained hydrodynamics. These observations are used to review data processing procedures and to recommend improved deployment methods, thus improving the precision, reliability, and confidence of EC measurements. Specifically, this study demonstrates that 1) the alignment of the time series based on maximum cross correlation improved the precision of EC flux estimations; 2) an oxygen sensor with a response time of <0.4 s facilitates accurate EC fluxes estimates in turbulence regimes corresponding to horizontal velocities < 11 cm s<sup>-1</sup>; and 3) the smallest possible distance (<1 cm) between the oxygen sensor and the ADV's sampling volume is important for accurate EC flux estimates, especially when the flow direction is perpendicular to the sensor's orientation.

6 Denotes Open Access content.

<sup>e</sup> Current affiliation: GM/LGM-Geochemistry and Metallogeny Laboratory, IFREMER, Plouzané, France.

<sup>h</sup> Current affiliation: LER/PC-Resources and Environment Laboratory, IFREMER, L'Houmeau, France.

<sup>l</sup> Current affiliation: Institute F.-A. Forel, University of Geneva, Geneva, Switzerland.

Corresponding author address: Daphne Donis, Max Planck Institute for Marine Microbiology, Celsiusstrasse 1, 28359 Bremen, Germany.  
 E-mail: ddonis@mpi-bremen.de

DOI: 10.1175/JTECH-D-14-00089.1

© 2015 American Meteorological Society

## 1. Introduction

Aquatic eddy correlation (EC) is an increasingly common technique to infer fluxes across the sediment–water interface in aquatic environments. The EC method is based on the simultaneous high-frequency measurement of the vertical velocity (normal to the local streamline) and the concentration of oxygen or other constituents (Berg et al. 2003). The method resolves the turbulent fluctuations in the benthic boundary layer (BBL), and the resulting time series data are averaged to obtain a mean benthic flux (Lorke et al. 2013). Performed in the turbulent boundary layer just above the sediment and assuming constant mean current velocities and oxygen concentrations (Holtappels et al. 2013), the measured flux represents the flux across the sediment–water interface averaged over an upstream-located footprint area (Berg et al. 2007).

Originally developed to resolve atmospheric fluxes in terrestrial environments (Baldocchi 2003), the EC application to the aquatic environment has shown promising results where conventional methods for benthic flux acquisition are difficult or impossible to apply (Glud et al. 2010; Hume et al. 2011; Long et al. 2012; Berg et al. 2013; Long et al. 2013). Despite the growing number of EC applications, there are still several unresolved issues, including deployment considerations (current direction, sensor spacing) as well as requirements on sensor response time. While these topics have been discussed in previous publications (McGinnis et al. 2008; Lorrain et al. 2010), their implications have not been fully assessed or investigated.

Indeed, among other constraints, the resolution of the instantaneous fluctuations of vertical velocity and oxygen concentration requires that 1) both measurements refer to exactly the same sampling volume and 2) all “flux carrying” eddies are properly resolved (Swinbank 1951; Foken et al. 2004). However, such requirements are not always fulfilled during in situ deployments. In practice, the oxygen sensor is located outside the sampling volume of the velocity measurement to avoid interference with the acoustic Doppler velocimeter (ADV). This physical separation, if not corrected for, can produce biased flux estimates (McGinnis et al. 2008; Lorrain et al. 2010; Billesbach 2011). Additionally, a potential bias can emerge due to the slower response time of the oxygen sensor relative to the response time of the ADV. Minimizing this potential bias requires a suitable time shift of both time series (by their cross correlation), but the loss of high-frequency fluctuations can still lead to errors (Eugster and Senn 1995; Aubinet et al. 2001). Although these issues were addressed theoretically, there exist no quantitative studies evaluating the potential effects of time shift and response times on eddy correlation flux estimates in the aquatic environment.

Here, we present the outcome of an international experimental workshop held in February 2012 at the Royal Netherlands Institute for Sea Research (NIOZ Yerseke) with the aim of exchanging ideas and experience among aquatic EC users. In this study, we address the effects of time shift and sensor response time on aquatic EC flux estimates. To this end, we performed experiments under controlled conditions in a large-scale laboratory flume combined with numerical modeling. From this, we developed a list of recommendations with respect to deployment and data processing to improve precision and reliability of EC flux measurements.

## 2. Materials and methods

### a. Flume setup

Eddy correlation measurements were performed in a large racetrack flume facility (Fig. 1) with a total length of 17.55 m, a width of 0.60 m, and a straight working section of 10.8 m. The water flow is generated by a conveyor belt system that uses a series of paddles to drive the flow [see Jonsson et al. (2006) for the flume hydrodynamic characteristics, referred to as a NIOO flume]. Ten days prior to the start of the experiments, cohesive sediment was collected from an intertidal flat at Kapelle Bank (Westerschelde estuary, The Netherlands; porosity  $\sim 0.7$ , organic carbon  $\sim 1.5$  wt%) (Middelburg et al. 1996; de Brouwer et al. 2000). Visible fauna were removed from the sediment that was then homogenized and deposited as a 5-cm-thick bottom layer, covering the working section of the flume (Fig. 1).

Seawater from the sampling site (salinity: 32) was used to fill the flume to a water depth of 30 cm (total water volume  $\sim 9$  m<sup>3</sup>). The temperature in the flume hall was kept constant at 17°C and the sediment was allowed to equilibrate for 10 days, before EC experiments were conducted. The flume was kept in darkness and low artificial light levels were only applied when instrumentation was added or changed; this ensured that no phototrophic growth took place in the flume. The temperature and O<sub>2</sub> concentrations in the flume water were continuously monitored with two optodes (4330F, Aanderaa), one located before the flow straighteners and the other optode was positioned at the end of the straight work section (Fig. 1).

### b. EC system

The EC system consisted of an ADV (Nortek) with two gain-adjustable, galvanically insulated amplifiers (McGinnis et al. 2011), each equipped with custom-built Clark-type O<sub>2</sub> microelectrodes (Revsbech 1989; Gundersen et al. 1998). The O<sub>2</sub> microelectrodes were calibrated against the air-saturated flume water and

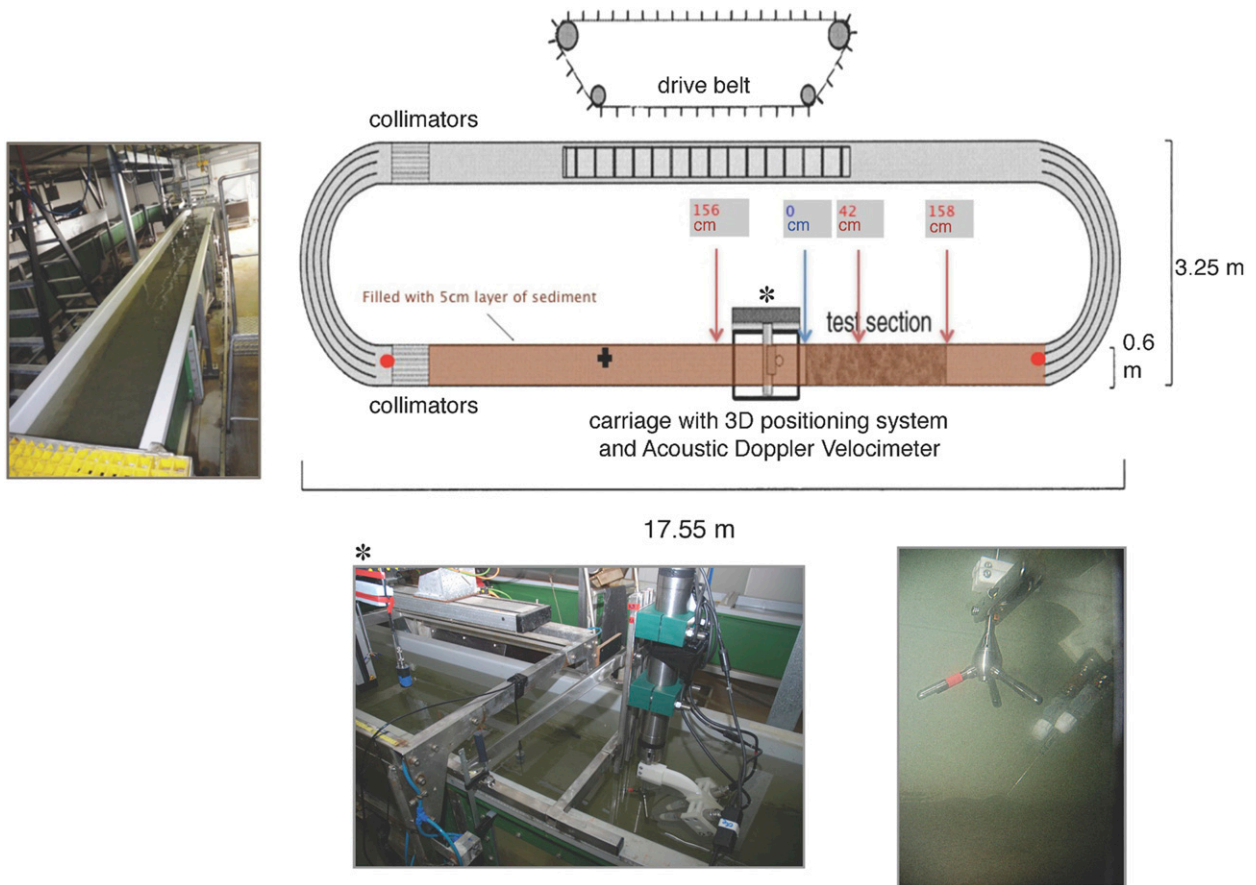


FIG. 1. Pictures of (top left), (bottom left) the racetrack flume facility at NIOZ-Yerseke and (bottom right) the EC system used for the experiments. (top right) A schematic of the flume: the dark brown shading indicates the straight working area, the red arrows indicate the location where the  $O_2$  microprofiles were performed, the blue arrow indicates the location where EC measurements were performed (position 0), the two red dots mark the position of the optodes for monitoring the  $O_2$  and temperature in the flume, and the cross indicates where the incubations were performed. Scheme adapted from Bouma et al. (2005).

anoxic flume water at the same temperature and salinity. The ADV sampling volume was located 15.7 cm below the probe and had an hourglass shape with diameters and height of 14 mm (Lohrmann et al. 1994). However, the sampling volume was assumed to be cylindrical with the same dimensions, from which the distance to the  $O_2$  microelectrode tip was defined. The EC system was battery powered and suitably grounded to avoid electrical noise. The ADV stem was positioned at 7-cm depth, while the amplifiers and oxygen sensors were almost completely submerged, with the tip of the oxygen sensors and the ADV sampling volume at a depth of 22 cm (see Fig. 1).

### c. Flux calculations

The  $O_2$  concentrations and velocities were sampled at 64 Hz and subsequently averaged (simple average) to 8 Hz to improve the signal quality while still resolving the high-frequency eddies (as evaluated from the

obtained velocity power density spectrum). Velocity spikes were removed and interpolated between neighboring data points (as described in Goring and Nikora 2002) with an ADV beam correlation threshold of 70% (Elgar et al. 2005).

The measured vertical velocity ( $w$ ) and  $O_2$  concentration ( $C$ ) can be separated into a fluctuating (prime) component and a mean (overbar) component as  $w = w' + \bar{w}$  and  $C = C' + \bar{C}$  (Reynolds 1895), respectively. The mean values were calculated by applying a moving average filter with a window length of 60 s (Moncrieff et al. 2004); this was sufficient to include the frequencies that contributed to the vertical flux (as discussed below). The  $O_2$  fluxes ( $F$ ) were calculated as  $F = \overline{w' C'}$  [see Lorke et al. (2013) for a complete derivation] over each 5-min interval, which represents a good balance between a clear data visualization and high temporal resolution.

To determine the time shift needed to align the time series,  $C'$  and  $w'$  were shifted relative to one another

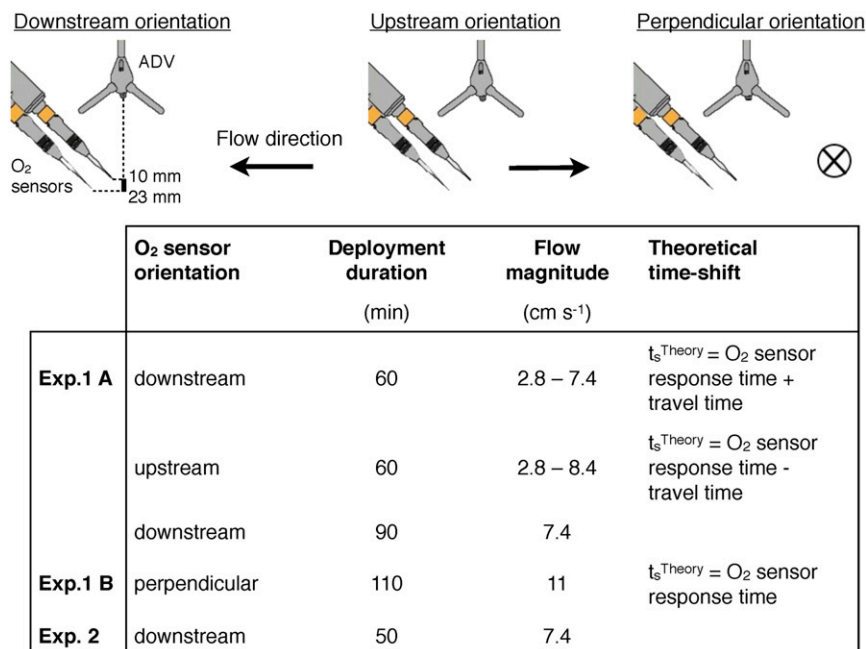


FIG. 2. (top) The EC system configuration and orientations used for the three experiments summarized here. The  $t_s^{\text{Theory}}$  is the expected displacement of the time series  $w'$  and  $C'$ , given by the sum of the O<sub>2</sub> sensors response and the travel time of the water parcel. An approximate estimation of the cross correlation needed for the alignment of the time series was calculated according to the  $t_s^{\text{Theory}}$  reported in the table.

using a 0.125-s step size (as defined by the 8-Hz sampling rate) over a window from 0 to 4 s for the respective 5-min interval (or sample window). The highest cross correlation (absolute value) in this window was used to calculate the EC flux for each sample. The statistical significance of the cross correlation was evaluated by calculating the probability of receiving the same correlation (i.e., the same flux) from a random dataset, by using the MATLAB 7.10.0 (R2010a) *corrcoef* function (Holtappels et al. 2013). The threshold for a significant flux was set to  $p < 0.05$ .

#### d. Experiment setup

Three specific flume experiments were conducted. Experiments 1A and 1B used two O<sub>2</sub> sensors with similar response times (90% response time;  $\tau_{90} = 0.35$  s; stirring sensitivity = ~1%). The sensors were positioned at different distances (10 mm, referred to as “proximal”; and 23 mm, referred to as “distant”) from the edge of the cylindrical ADV sampling volume. The EC system was oriented downstream, upstream, or perpendicular to the flow direction (Fig. 2): these three configurations were expected to result in distinct and different time shifts ( $t_s$ ) for the optimal correlation between  $w'$  and  $C'$ .

Experiment 2 was conducted to compare two O<sub>2</sub> sensors with different response times of 0.35 and 3.00 s

(for the latter, stirring sensitivity = ~0%) (Figs. 3b,c). Both sensors were positioned at 10-mm distance from the velocity sampling volume. See Fig. 2 for the deployment summary.

#### e. O<sub>2</sub> microsensor profiles and chamber measurements

Diffusive O<sub>2</sub> uptake (DOU) was determined from O<sub>2</sub> profiles across the sediment–water interface obtained using an O<sub>2</sub> microelectrode (tip diameter of 50  $\mu\text{m}$  and  $\tau_{90} < 5$  s) positioned by a motor-controlled micromanipulator. DOU was determined from the linear concentration gradient just beneath the water–sediment interface using Fick’s first law of diffusion (Glud 2008). The porosity at the sediment–water interface was assumed to be 0.7, and the molecular diffusion of O<sub>2</sub> was calculated from temperature and salinity based on Soetaert et al. (2012). Measurements were conducted at three different positions in the working section of the flume (0.4 and 1.5 m downstream, and 1.5 m upstream from the EC device) and at three flow velocities (18, 7.1, and 2.7 cm s<sup>-1</sup>). Furthermore, the total oxygen uptake (TOU) of the sediment was determined via chamber incubations, which were performed 4 m upstream from the EC system (Fig. 1). Three acrylic chambers ( $\varnothing$ : 11 cm; height: 10 cm) were gently pushed into the

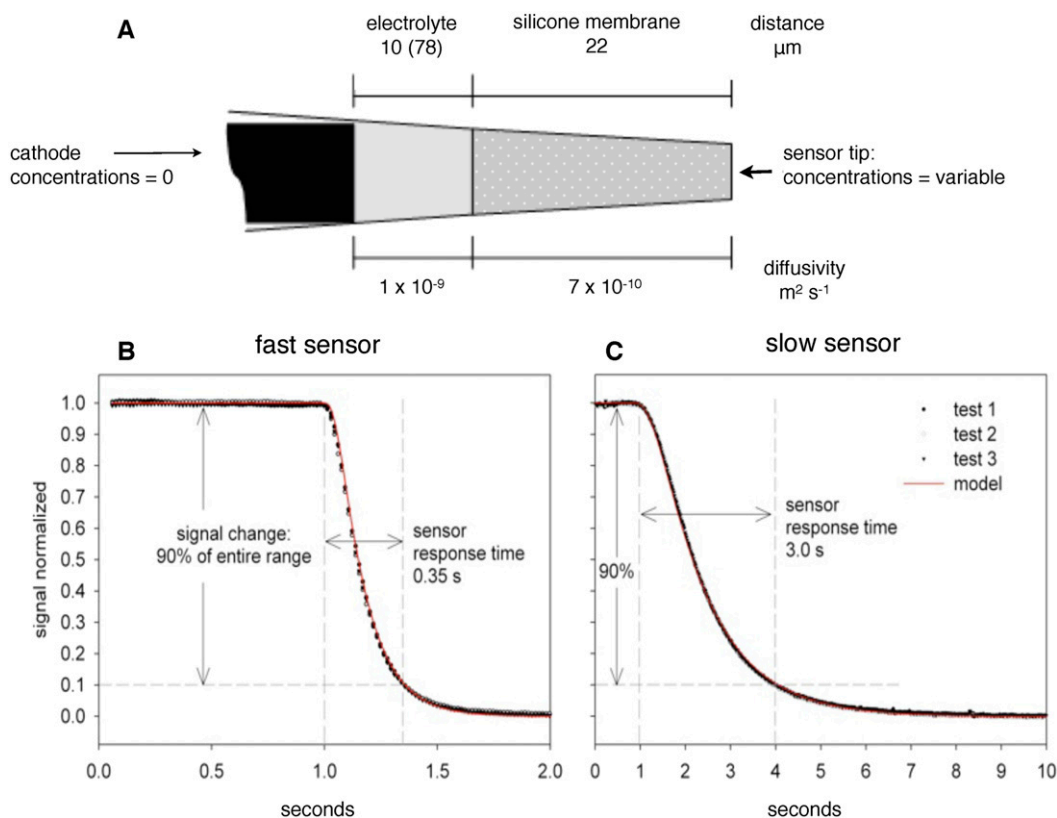


FIG. 3. (a) Schematic drawing of an O<sub>2</sub> microsensor, showing the dimensions and diffusivities as used in the numerical model. (b),(c) Response times of a slow (3.00 s) and a fast (0.35 s) O<sub>2</sub> microelectrodes used for experiment 2 in the flume. The response time is defined as the time required to  $\tau_{90}$ .

sediment, and the O<sub>2</sub> concentration was continuously logged during the ~20-h incubations (Firesting oxygen optode, PyroScience GmbH). TOU rates were computed by linear regression of the O<sub>2</sub> time series as a function of time. The O<sub>2</sub> levels never declined more than 20% from the initial value during the incubations. Both TOU and DOU measurements were performed 4–8 days after the sediment and filtered seawater had been introduced to the flume.

#### f. Numerical model of a Clark-type microelectrode

To further assess the effect of sensor response time, we developed a numerical model of an oxygen microsensor using the finite element program COMSOL Multiphysics 4.3 (<http://www.comsol.com>). The O<sub>2</sub> flux to the cathode was described using a one-dimensional diffusion model with two domains, membrane and electrolyte (Fig. 3a) (Glud et al. 2000), with O<sub>2</sub> diffusivities of 0.69 and 1.00 × 10<sup>-9</sup> m<sup>2</sup> s<sup>-1</sup>, respectively (Gundersen et al. 1998). The maximum element size in either domain was 0.05 μm. The concentration at the cathode was set to zero, whereas the input concentration at the tip was determined by a prescribed time series of

realistic O<sub>2</sub> concentrations. The oxygen distribution across domains was calculated using a time-dependent solver. The output concentrations  $C_{\text{out}}$  of the sensor model were calculated from the modeled flux at the cathode  $J_{\text{cath}}$  (both time dependent) and multiplied by a calibration factor derived from the ratio of mean input concentrations at the sensor tip  $\overline{C_{\text{in}}}$  and the respective mean flux at the cathode:

$$J_{\text{cath}}(t) \frac{\overline{C_{\text{in}}}}{J_{\text{cath}}} = C_{\text{out}}(t). \quad (1)$$

A first step was to assess the effect of sensor response time on the fluxes measured during experiment 2. Therefore, we applied the model to simulate the O<sub>2</sub> flux as recorded by the fast ( $\tau_{90} = 0.35$  s) and slow ( $\tau_{90} = 3.00$  s) responding sensors, as in the experiment. The physical dimensions of the simulated slow and fast sensors were based on the dimensions of the custom-built sensors (Fig. 3a). The response time of the sensor models was estimated by applying abrupt changes of O<sub>2</sub> concentrations at their tip. The model was validated by comparing modeled and measured response times (Figs. 3b,c).

Subsequently, in order to investigate the potential bias of especially the fast sensor ( $\tau_{90} = 0.35$  s), we generated an artificial time series of  $O_2$  oscillations and used it as input into the numerical simulation. To approximate realistically high-frequency  $O_2$  oscillations, we used a time series of measured vertical velocity fluctuations and multiplied the values with the ratio of the standard deviations of  $C'$  over  $w'$  [ $\text{std}(C')/\text{std}(w')$ ] in order to scale down the amplitude, so that the standard deviation matches those of the measured  $O_2$  concentration fluctuations. Afterward, the time series was multiplied by  $-1$  for a maximum negative correlation with the vertical velocity fluctuations (i.e., a downward flux).

For our model results, the instantaneously responding sensor was considered to be the baseline flux, that is, the flux obtained considering no distance or response time difference between velocity and  $O_2$  concentration measurements for experiment 2. With the same approach, we were also able to simulate a fast-response time sensor of 0.1 s.

#### g. Theoretical correction with frequency-dependent dampening correction

The sensor response time can potentially dampen the signal from turbulent oxygen fluctuations, with increased dampening occurring at higher frequencies. This leads to a signal loss that can be estimated by spectral analysis (McGinnis et al. 2008). One procedure is to apply a frequency-dependent transfer function (Eugster and Senn 1995; Gregg 1999) to the  $O_2$ -velocity cospectrum  $S_{O_2}^{\text{obs}}$  ( $\text{mmol m}^{-2} \text{s}^{-1}$ ) to arrive at an enhanced cospectrum:

$$S_{O_2}^{\text{Corr}}(\omega) = (1 + \omega^2 \tau^2) S_{O_2}^{\text{obs}}, \quad (2)$$

where  $\omega$  is the wavenumber [ $\omega = 2\pi f$ , where  $f$  is frequency (Hz)] and  $\tau$  (s) is the  $1/e$  ( $\sim 63\%$ ) response time. We integrated the enhanced cospectra to estimate the signal loss (expressed as a percentage of the flux) resulting from the slower sensor response time. The integration of the enhanced cospectrum, however, should only be applied up to the highest frequency of the eddy contributions [e.g., estimated for a logarithmic boundary layer as in Table 1 in Lorrai et al. (2010)] and not beyond this point, as the transfer function also enhances the noise.

### 3. Results

#### a. EC measurements: Time-shift effect on measured $O_2$ fluxes

We compared the frequency spectra of the vertical component of the flow, measured for perpendicular and downstream orientation at the same flow velocity. These

were nearly identical (data not shown), excluding any anomaly potentially induced by the submerged instrument (e.g., flume-wall effect).

To illustrate the effect of the time shift on the EC fluxes, the results for experiments 1A and 1B are presented, including estimated time shifts and cross-correlation  $p$  values over the entire deployments (Figs. 4a–d). Different effects of time shift on the EC flux were observed according to sensor positions and orientations with respect to the flow direction (Figs. 4a–d). The calculated time shift ( $t_s$ ) required for maximum correlation between  $w'$  and  $C'$  for both sensors increased with decreasing flow velocity (Fig. 4b). As expected (and according to Fig. 2), the sign of  $t_s$  reversed when shifting the sensor orientation from downstream to upstream (gray area in Fig. 4b). Furthermore, the  $O_2$  sensor proximal to the velocity sampling volume had a less variable  $t_s$  compared to the sensor positioned at 23 mm, particularly under conditions of low flow velocity and perpendicular sensor orientation (Fig. 4b).

Oxygen fluxes measured during experiments 1A and 1B are listed in Table 1. On average the time-shift correction leads to an increase in the  $O_2$  flux by  $\sim 40\%$  and  $\sim 30\%$  for the proximal and distant sensors, respectively. No significant difference is observed between the average fluxes from the two  $O_2$  sensors (Table 1). However, as shown from Figs. 4c,d, the significance of the cross correlations increase substantially after applying the time shift, except for the 23-mm distant sensor case at perpendicular orientation. The most statistically robust correlations (with or without time-shift correction) are observed for the downstream orientation, compared to the upstream and perpendicular ones (Figs. 4c,d). The observed divergence between fluxes obtained for different sensors' orientations suggests that the applied time-shift correction procedure does not completely compensate for the biases related to the flow direction (i.e., the signal loss due to the undersampling of contributing eddies).

Reference measurements obtained by microprofiles and chamber incubations were carried out on different days at different positions in the flume and showed no significant differences (Table 2; Fig. 5), suggesting that the sediment diagenetic activity was in steady state throughout the duration of EC measurements. No significant diurnal variations of  $O_2$  benthic fluxes were observed (the flume hall was kept dark except during the experiment setup), and  $O_2$  concentrations along the water column and air–water exchanges appeared to be steady.

The closest agreement between EC fluxes and reference measurements ( $\text{TOU} = -12 \pm 4$ ;  $\text{DOU} = -8 \pm 2$   $\text{mmol O}_2 \text{m}^{-2} \text{day}^{-1}$ ; Table 2) occurs when the EC

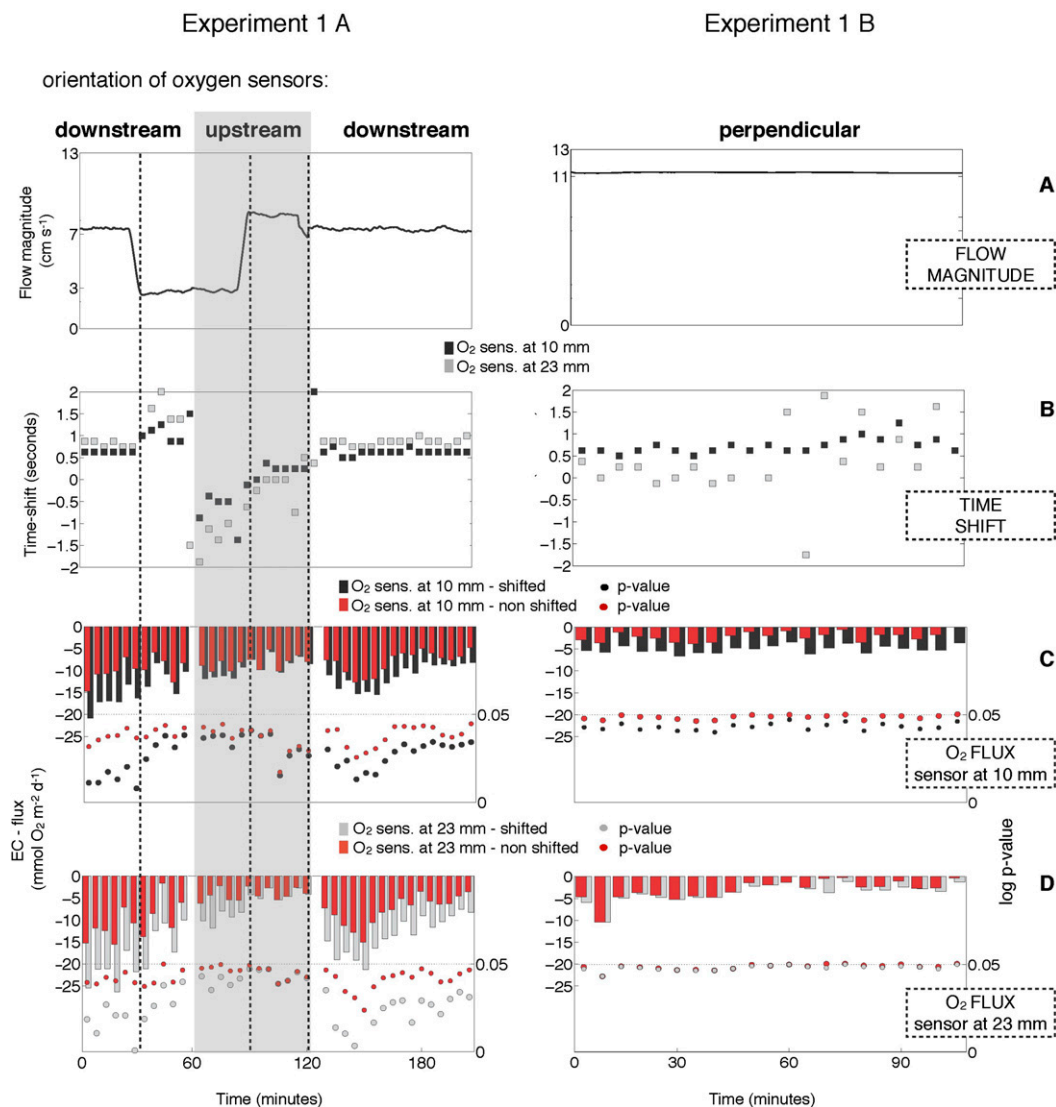


FIG. 4. Results for (left) experiment 1A and (right) experiment 1B. (a) Flow magnitude of the flume. (b) Time shift calculated for the maximum cross correlation (absolute value) on a 5-min sample window for sensor at 10 mm (black) and sensor at 23 mm (gray). (c) The  $O_2$  fluxes for a sensor at 10 mm calculated before (red bars) and after (black bars) time-shift correction;  $p$  values (dots) corresponding to shifted and nonshifted fluxes are reported with the same color code. (d) The  $O_2$  fluxes for sensor at 23 mm calculated before and after time-shift correction (red and gray bars, respectively), and  $p$  values corresponding to shifted and nonshifted fluxes (same color code). Gray area corresponds to upstream orientation of the  $O_2$  sensors and the vertical dashed lines to the change in flow magnitude.

instrument is aligned in the downstream orientation, without applying the time-shift correction (Table 1). However, for the other flow orientations (upstream and perpendicular), the agreement between EC fluxes and reference measurements improves by applying the time-shift correction as shown in the following section.

#### b. Analysis on single EC sample windows

The cross-correlation functions between the velocity and  $O_2$  time series are shown in Figs. 6a–c for each positioning of the sensors. This allows for evaluating how

the time-shift correction influences EC fluxes. The maximum of the cross-correlation function defines the observed time shift ( $t_s^{Obs}$ ). There is a marked difference in the shape of the cross-correlation functions between the different flow directions. When the  $O_2$  sensors are located downstream, the cross-correlation function has a sharp, well-defined maximum (observed time shifts of 0.7 and 0.9 s for the 10- and 23-mm sensor spacing, respectively; Fig. 6a). In contrast, and as expected, when the sensors are located upstream, the maximum cross correlation occurs for smaller time shifts ( $\sim 0.4$  s).



TABLE 2. Flume benthic oxygen fluxes obtained between 8 and 14 Feb 2012 at different positions and flow speed by microsensing and chamber incubations (EC flux results in Table 1 refer to 14 Feb 2012).

Date	Flow magnitude ( $\text{cm s}^{-1}$ )	Position (cm)	DOU ( $\text{mmol O}_2 \text{m}^{-2} \text{day}^{-1}$ )
10 and 11 Feb	18	158	$9.8 \pm 1.2; n = 8$
13 Feb	7.1	158	$8.0 \pm 0.9; n = 3$
12 Feb	2.7	158	$7.6 \pm 0.4; n = 4$
	2.7	-156	$8.4 \pm 1.0; n = 3$
	2.7	40	$7.8 \pm 1.2; n = 3$
	2.7	158	$7.3; n = 1$
			TOU ( $\text{mmol O}_2 \text{m}^{-2} \text{day}^{-1}$ )
8–14 Feb		(see Fig. 1)	$12 \pm 2; n = 3$

ultrafast = 0.1 s, fast = 0.35 s, and slow = 3.00 s). We compared the fluxes obtained with different response times to the fluxes obtained by an ideal (i.e., instant response) sensor (Table 3). The  $\text{O}_2$  flux is reduced by 45% and 65% for the fast and slow  $\text{O}_2$  sensors, respectively, while an ultrafast sensor with a 0.1-s response time would have a flux loss of 16%. Note that these results are specific to a flow velocity of  $7.4 \text{ cm s}^{-1}$  and the given flume conditions.

#### d. Theoretical correction with frequency-dependent transfer function

The  $\text{O}_2$  spectra can be “rebuilt” to account for signal loss due to the sensor response time (McGinnis et al. 2008), knowing that the slower response time dampens the turbulent fluctuations, with increased dampening occurring at higher frequencies. Therefore, we applied the correction using Eq. (2) to the dataset (experiment 2) utilizing the 3-s response time sensor.

The calculated correction is shown in Fig. 7 as a function of the frequency of the  $\text{O}_2$  oscillations.

The spectral corrections become quite substantial when sampling high frequencies with a slow sensor. However, the turbulent eddy contributions decrease with increasing frequency (as shown in Fig. 8 and discussed below), so while these corrections seem large, they are less (but still) significant when rebuilding the cospectra.

Figure 7b shows the flux underestimation for the  $7.4 \text{ cm s}^{-1}$  case (experiment 2) as a function of sensor response time, which was derived by multiplying the  $\text{O}_2$  spectra with the correction factor as a function of frequency. The average fluxes were calculated for each hypothetical response time by integrating the flux between the limits assumed to be defined by the flux-contributing range (5–0.1 Hz; see Lorrai et al. 2010). The results are not sensitive to the lower-frequency

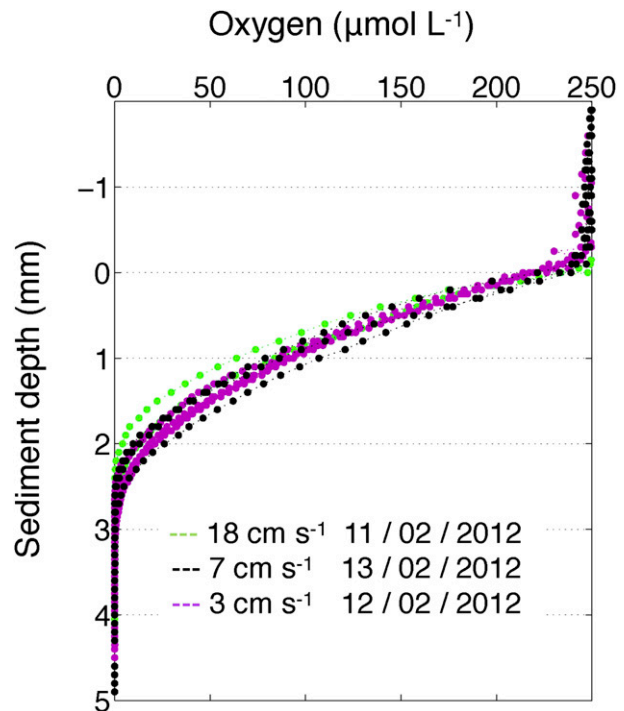


FIG. 5. The  $\text{O}_2$  profiles performed in the flume at 158 cm (see Fig. 1) over 4 days at different flow velocities. The  $\text{O}_2$  penetration depth ranged between 2.5 and 3 mm below the sediment-water interface.

integration limit, as the correction quickly decreases for lower frequencies; however, it is very sensitive to the high-frequency limit. The correction has a tendency to amplify high-frequency noise, so that integration beyond the high-frequency limit may introduce artefacts. Therefore, this example is only valid for the  $7.4 \text{ cm s}^{-1}$  case, as the flux-contributing eddy range (including the inertial subrange) will shift with changing velocity. For the case of the 3-s response time, we estimate that a 67% correction would be needed. This is very close to the value obtained from the  $\text{O}_2$  sensor model results (Table 3).

## 4. Discussion

The assessment of turbulent benthic solute exchanges with an EC system requires instantaneous measurements of velocities and a scalar at the same point. This is practically impossible to achieve with the currently available instrumentation, that is, the combination of an ADV and a fast-responding sensor (here, we examined the most used Clark-type microelectrode for dissolved  $\text{O}_2$  measurements). Previous work on aquatic EC measurements (McGinnis et al. 2008; Lorrai et al. 2010) has described how the flux measurements are systematically biased due to the different response time and the physical distance of the sensors. The authors introduced

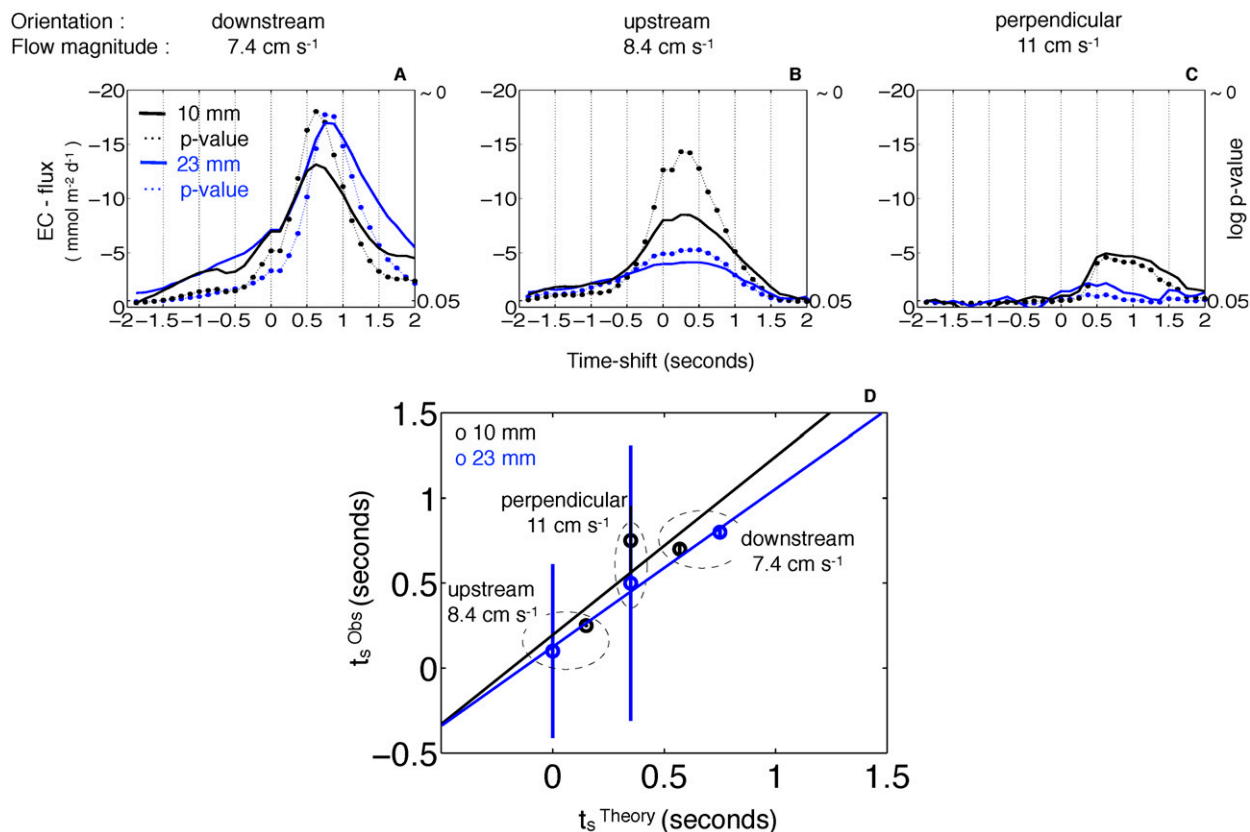


FIG. 6. (a)–(c) Cross-correlation functions between the velocity and O<sub>2</sub> time series (solid line) and respective *p* values (dotted line), for sensors positioned at 10 and 23 mm from the center of velocity sampling volume (black and blue, respectively). Data are shown for one representative sample window for each orientation at comparable flow velocities. (d) Average and error bars of observed time-shift ( $t_s^{Obs}$ , time-shift of  $w'$  vs  $C'$  needed to achieve the maximal correlation) vs the predicted theoretical time-shift ( $t_s^{Theory}$ , sum of traveling time and sensor response time) for each orientation at comparable velocities, for experiments 1A and 1B. The lines indicate linear regression.

correction procedures, however, that were based only on theoretical assumptions. We therefore designed ad hoc experiments in controlled environments (flume tank) and a model of a Clark-type microelectrode to systematically study the errors caused by sensor displacement and response times and to evaluate the correction procedures at hand.

*a. Time shift, sensor displacement, and flow direction*

By analyzing EC measurements in the well-constrained conditions of a large-scale flume facility, we could assess O<sub>2</sub> fluxes for different sensor positions (i.e., orientation and distance of O<sub>2</sub> sensors with respect to the center of the ADV sampling volume) at different flow magnitudes and directions. The dependency of estimated fluxes on sensor position is an aspect that has not been addressed in aquatic EC studies. While some variability of measured O<sub>2</sub> fluxes is expected to occur due to natural hydrodynamic conditions (Holtappels et al. 2013) and bottom heterogeneity (e.g., Rheuban and Berg 2013), our results indicate that some of the flux

variability is also related to the orientation of the sensor with respect to the flow direction. This effect is not easily resolved in natural environments, where a highly intermittent flow field and spatial variations may mask the artifacts in benthic flux estimates. However, when averaged over longer time scales, the average flux might also be less sensitive to these potential issues.

Results from the flume investigation here reveal that when the flow is parallel to the sensor (i.e., downstream or

TABLE 3. Model prediction of a slow (3.00 s), fast (0.35 s), ultrafast (0.1 s), and artificial and infinitely fast (0.0 s) O<sub>2</sub> sensor signal, and percentage of loss flux as referred to the 0-s response.

Sensor response time (s)	Time shift for max cross correlation (s)	Flux modeled (mmol O <sub>2</sub> m <sup>-2</sup> day <sup>-1</sup> )	Loss of flux (%)
0 (artificial)	0.0	-45	0
0.10	0.2	-38	15
0.35	0.4	-20	45
3.00	1.3	-16	65

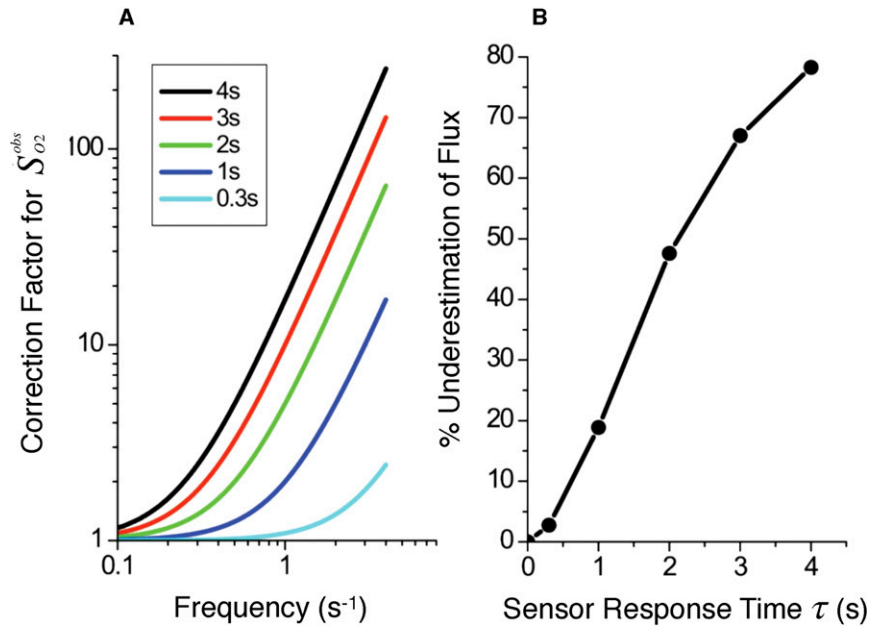


FIG. 7. (a) The frequency-dependent correction factor ( $1 + \omega^2\tau^2$ ) applied to the  $O_2$  spectrum. (b) Underestimation of the flux as a function of sensor response time.

upstream orientation; Fig. 2), the turbulent structures pass the  $O_2$  and velocity sensor with a delay that depends on the distance between sampling positions for  $w'$  and  $C'$  and the response time of the  $O_2$  sensor. However, an increasing distance between sampling volumes lowers the probability of sampling the same eddy structure, as evident by the more statistically significant correlations between  $w'$  and  $C'$  obtained in our experiments for the proximal sensor (10 vs 23 mm). Thus, it is advantageous to position the  $O_2$  sensor as close as possible ( $<1$  cm) to the edge of the velocity sampling volume, but taking care that it does not enter the sampling volume. If larger diameter sensors are used, these new dimensions must be considered with respect to the potential interference.

If all the orientations of the  $O_2$  sensors with respect to the flow are considered for the flux average (equal deployment time of 60 min for downstream, upstream, and perpendicular), then we observed similar EC fluxes compared to chambers and microprofile estimates, only after applying the time-shift correction (EC =  $-9 \pm 4$ ; TOU =  $-12 \pm 4$ ; DOU =  $-8 \pm 2$  mmol  $O_2$  m $^{-2}$  day $^{-1}$ ).

However, the best agreement with TOU measurements occurs when the EC instrument is aligned downstream with or without time-shift correction, (EC shifted =  $-16 \pm 3$ ; EC nonshifted =  $-10 \pm 2$  mmol  $O_2$  m $^{-2}$  day $^{-1}$ , for sensor distance of 10 mm), while when the orientation is upstream, the flux magnitude and the significance of the correlation decrease substantially. A flux magnitude decrease for the upstream orientation was observed for both proximal and distant  $O_2$  sensors and

holds true after applying the time-shift correction (EC shifted =  $-9 \pm 1$  mmol; EC nonshifted =  $-8 \pm 1$  mmol  $O_2$  m $^{-2}$  day $^{-1}$ , for sensor distance of 10 mm). The weaker correlation between  $w'$  and  $C'$  at upstream orientations and the reduced effectiveness of the alignment procedure could be caused by the sensors and amplifiers affecting the flow and the turbulent structures. Finally, the perpendicular orientation results in underestimated fluxes by 70% compared to fluxes measured when the  $O_2$  sensors are oriented downstream (EC shifted =  $-5 \pm 1$ ; EC nonshifted =  $-2 \pm 1$  mmol  $O_2$  m $^{-2}$  day $^{-1}$ , for

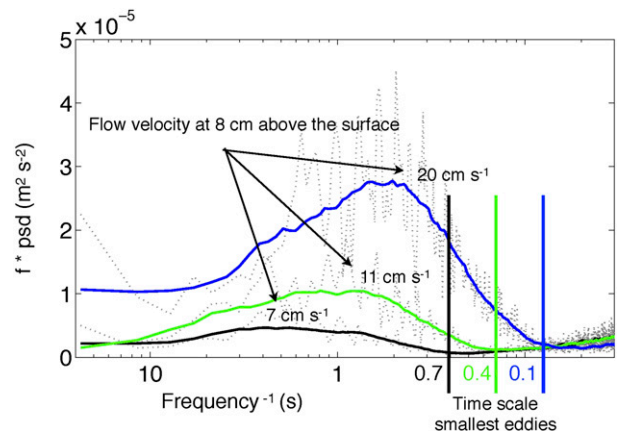


FIG. 8. Variance-preserving spectra of  $w$  corresponding to flow velocities of 7 (black), 11 (green), and 20 cm s $^{-1}$  (blue) measured in the flume at 8 cm above the surface. The curves, smoothed by adjacent averaging over 50 data points, indicate for each flow field the lifetime range of turbulent eddies.

a sensor distance of 10 mm). Flow directions perpendicular to the sensors line are indeed more challenging, given the higher probability for the ADV and O<sub>2</sub> sensors of measuring decoupled signals. Moreover, at perpendicular orientation, the travel time alignment is not applicable, so that the highest frequencies contributing to the flux (i.e., eddy lengths smaller than the distance between the sensors) are more likely to be missed. Clearly, the more robust correlations obtained for the proximal sensor confirm that a closer distance reduces this decoupling effect. Note, however, that such a poor correlation is not necessarily expected in the field, because of a much larger variability in the magnitude and direction of the flow. However, these results do suggest that the instrument should ideally be aligned in the main direction of the flow.

Given that flume walls have a negligible boundary layer thickness (~1 cm) and we did not observe any anomaly in the velocity frequency spectra during the entire experiment, we exclude the possibility that the poor cross correlation at perpendicular orientation is caused by sidewall effects. However, the dimensions of the racetrack flume are appropriate only for the scales of the hydrodynamic processes corresponding to the higher-frequency turbulent structures, which represent a restricted range of field applications.

In summary, the flow direction appears as an important factor influencing EC flux measurements. The time-shift correction does not lead to a uniform flux estimations between downstream, upstream, and perpendicular orientations, especially because the latter case cannot be fully corrected because of the undersampling of flux-carrying eddies. For downstream configurations, the time-shift correction can correct this bias, although increasing displacements increase the mismatch of the spatial overlay of corresponding velocity–concentration pairs and may constitute a weak point of this method, especially under nonuniform flow conditions. However, if all three orientations from our flume data are equally considered in the flux average, then the time-shift correction improves the confidence and precision of the obtained flux estimation up to 30% (Table 1). Applying a time shift is thus a convenient procedure, and it was confirmed that it corresponds closely to the sum of traveling time and O<sub>2</sub> sensor response time (discussed below) for the case of downstream and upstream orientation of the EC system.

#### *b. Flux underestimation due to microsensor response time*

Similar to what has been assessed for the atmospheric application of EC (see Foken et al. 2012), we demonstrate that for aquatic EC, corrections must be introduced when the maximum frequency response of a sensor is less than the highest frequency of the

turbulent eddies responsible for the flux (McGinnis et al. 2008). By applying a 1D model to simulate O<sub>2</sub> diffusion in a microsensor and imposing a vertical velocity signal with the same amplitude of the O<sub>2</sub> signal, we were able to estimate the fluxes measured by microsensors with different response times. The simulations showed that an O<sub>2</sub> sensor with a 3.00-s response time (thus, 10 times slower than sensors usually used for EC measurements) leads to an underestimation of 65% of the true flux (i.e., no response time and no signal dampening) and a sensor with a 0.10-s response time results in a 15% loss for the conditions evaluated (7.4 cm s<sup>-1</sup>). This indicates that high-frequency signal loss, intrinsic to any electrochemical electrode measurement, cannot be corrected by the time-shift procedure alone. The dampening effect on vertical solute transport estimations by EC can be significant, depending on the frequency of the turbulent processes involved. At our flume conditions, a sensor with a  $\tau_{90}$  of 0.4 s would resolve nearly the complete flux-contributing eddy ranges for a flow velocity of <11 cm s<sup>-1</sup> (measured at 8-cm height); however, the sensors are not sufficiently fast for flow velocities >20 cm s<sup>-1</sup> (Fig. 8).

In summary, at lower flow velocities, the signal loss is less relevant because there are fewer flux contributions from high frequencies. Conversely, the portion of missed turbulent contributions becomes increasingly relevant with slower-responding O<sub>2</sub> sensors and increasing velocity.

Using the theoretical time scales of flux-contributing eddies (approximated, e.g., in Lorrai et al. 2010), it is possible to have an a priori estimate of the spectral range that is affected by sensor response time and correct it with the theoretical approach described here. This procedure is therefore recommended when turbulence regimes appear critical with respect to the O<sub>2</sub> sensor response time.

## 5. Conclusions and recommendations

Our flume experiments revealed that a closer distance between the ADV sampling volume and the O<sub>2</sub> sensor leads to more statistically significant correlations between  $w'$  and  $C'$ , thus to a better EC flux estimation. We showed that applying a time-shift correction improves the precision of the EC flux estimates and that the correction is particularly successful when the O<sub>2</sub> sensors are oriented downstream.

We found that when the current direction approaches perpendicular (Fig. 2) to the O<sub>2</sub> sensor-to-measuring volume line, then the likelihood that the signals are decoupled increases compared to other current directions (i.e., upstream or downstream). The effect is particularly exaggerated when the physical distance

between the sampling locations is increased, which translates into poor correlations and underestimated fluxes. For example, a somewhat high turbulence regime (e.g., friction velocity  $> 0.01 \text{ m s}^{-1}$ ) combined with a sensor separation distance of 2 cm can lead to flux underestimation approaching 80%. Therefore, if the flow direction is expected to change during the deployment of an EC system, then the  $\text{O}_2$  sensor tip distance from the velocity sampling volume should be as small as possible ( $< 1 \text{ cm}$ ). Accordingly, one may also consider discarding the fluxes obtained for orientations other than downstream/upstream.

Slow sensors may also lead to signal loss. We demonstrate how the response time of the  $\text{O}_2$  sensor is crucial to capture the  $\text{O}_2$  fluctuations defined by turbulent processes that ultimately govern the benthic  $\text{O}_2$  fluxes. Therefore, the error associated with a response time of the  $\text{O}_2$  sensor depends on the turbulence levels, which define the eddy time scales that contribute to the vertical flux.

The spatial scale of this experiment setup is not entirely representative of most natural environments, where advective processes can lead to extremely variable and complex interactions with the seafloor (e.g., unsteady advection due to internal or surface gravity waves). Thus, compared to EC measurements in natural systems, our results are likely to be more sensitive to signal losses at the higher frequencies of the inertial subrange, resulting in flux underestimations.

Nevertheless, a greater underestimation of the flux is expected for any EC application when using a sensor with a response time of more than 0.2 s (the usual recommended  $\tau_{90}$  for an EC measurement). In our case, we already observed a 15% signal loss from a sensor with  $\tau_{90} = 0.1 \text{ s}$  for velocities of  $7.4 \text{ cm s}^{-1}$ ; thus, the reliability of the EC measurements in flows much higher than  $20 \text{ cm s}^{-1}$  (i.e., with frequency ranges  $> 10 \text{ Hz}$ ) should be carefully considered. In settings with lower current speeds on the order of  $2\text{--}10 \text{ cm s}^{-1}$ , this effect is of less importance. Generally, it is beneficial to assess the  $\text{O}_2$  sensor response time in relation to the expected flow prior to any in situ deployment.

Here, for the first time, we systematically investigate the bias in aquatic EC measurements resulting from 1) the physical separation between the  $\text{O}_2$  sensor tip and the velocity sampling volume and 2) the  $\text{O}_2$  sensor response time. The results promote awareness of these potential sources of measurement artifacts for field measurements, and allowed us to assess a potential EC flux underestimation resulting from these factors and to provide guidelines for deployment design and data treatment.

*Acknowledgments.* We thank the staff at NIOZ (Yerseke, the Netherlands) and Landau University for

providing technical support in the use of the climate room and flume facilities, and Anni Glud for manufacturing the microelectrodes. Support for this work was provided by the Max Planck Society, the EU Seventh Framework Programme “SENSEnet” (PITN-GA-2009-237868), the Helmholtz Alliance “ROBEX,” the EU project “HYPOX” (Grant 226213), the Netherlands Organisation for Scientific Research (NWO-VIDI Grant 864.08.004 to FJRM), the Research Foundation—Flanders (FWO-Odyssée Grant G.0929.08 to FJRM), the University of Landau, the Department of Biology at Southern Danish University, and the Nordic Center for Earth Evolution (NordCEE; Grant DNRFF 53).

## REFERENCES

- Aubinet, M., B. Chermanne, M. Vandenhaute, B. Longdoz, M. Yernaux, and E. Laitat, 2001: Long term carbon dioxide exchange above a mixed forest in the Belgian Ardennes. *Agric. For. Meteorol.*, **108**, 293–315, doi:10.1016/S0168-1923(01)00244-1.
- Baldocchi, D. D., 2003: Assessing the eddy covariance technique for evaluating carbon dioxide exchange rates of ecosystems: Past, present and future. *Global Change Biol.*, **9**, 479–492, doi:10.1046/j.1365-2486.2003.00629.x.
- Berg, P., H. Røy, F. Janssen, V. Meyer, B. B. Jørgensen, M. Huettel, and D. de Beer, 2003: Oxygen uptake by aquatic sediments measured with a novel non-invasive eddy-correlation technique. *Mar. Ecol. Prog. Ser.*, **261**, 75–83, doi:10.3354/meps261075.
- , —, and P. L. Wiberg, 2007: Eddy correlation flux measurements: The sediment surface area that contributes to the flux. *Limnol. Oceanogr.*, **52**, 1672–1684, doi:10.4319/lo.2007.52.4.1672.
- , and Coauthors, 2013: Eddy correlation measurements of oxygen fluxes in permeable sediments exposed to varying current flow and light. *Limnol. Oceanogr.*, **58**, 1329–1343.
- Billesbach, D. P., 2011: Estimating uncertainties in individual eddy covariance flux measurements: A comparison of methods and a proposed new method. *Agric. For. Meteorol.*, **151**, 394–405, doi:10.1016/j.agrformet.2010.12.001.
- Bouma, T. J., M. B. De Vries, E. Low, G. Peralta, I. C. Táncoz, J. Van De Koppel, and P. M. J. Herman, 2005: Trade-offs related to ecosystem engineering: A case study on stiffness of emerging macrophytes. *Ecology*, **86**, 2187–2199, doi:10.1890/04-1588.
- de Brouwer, J. F. C., S. Bjelic, E. de Deckere, and L. J. Stal, 2000: Interplay between biology and sedimentology in a mudflat (Biezelingse Ham, Westerschelde, The Netherlands). *Cont. Shelf Res.*, **20**, 1159–1177, doi:10.1016/S0278-4343(00)00017-0.
- Elgar, S., B. Raubenheimer, and R. T. Guza, 2005: Quality control of acoustic Doppler velocimeter data in the surfzone. *Meas. Sci. Technol.*, **16**, 1889–1893, doi:10.1088/0957-0233/16/10/002.
- Eugster, W., and W. Senn, 1995: A cospectral correction model for measurement of turbulent  $\text{NO}_2$  flux. *Bound.-Layer Meteorol.*, **74**, 321–340, doi:10.1007/BF00712375.
- Foken, T., M. Göckede, M. Mauder, L. Mahrt, B. D. Amiro, and J. W. Munger, 2004: Post-field data quality control. *Handbook of Micrometeorology: A Guide for Surface Flux Measurement and Analysis*, X. Lee, W. J. Massman, and B. E. Law, Eds., Atmospheric and Oceanographic Sciences Library, Vol. 29, Kluwer Academic, 181–208.

- , M. Aubinet, and R. Leuning, 2012: The eddy covariance method. *Eddy Covariance: A Practical Guide to Measurement and Data Analysis*, M. Aubinet, T. Vesala, and D. Papale, Eds., Springer Atmospheric Sciences, Springer, 1–19.
- Glud, R. N., 2008: Oxygen dynamics of marine sediments. *Mar. Biol. Res.*, **4**, 243–289, doi:10.1080/17451000801888726.
- , J. K. Gundersen, and N. B. Ramsing, 2000: Electrochemical and optical oxygen microsensors for in situ measurements. In *Situ Monitoring of Aquatic Systems: Chemical Analysis and Speciation*, J. Buffle and G. Horvai, Eds., John Wiley and Sons, Ltd., 19–73.
- , P. Berg, A. Hume, P. Batty, M. E. Blicher, K. Lennert, and S. Rysgaard, 2010: Benthic O<sub>2</sub> exchange across hard-bottom substrates quantified by eddy correlation in a sub-Arctic fjord. *Mar. Ecol. Prog. Ser.*, **417**, 1–12, doi:10.3354/meps08795.
- Goring, D. G., and V. I. Nikora, 2002: Despiking acoustic Doppler velocimeter data. *J. Hydraul. Eng.*, **128**, 117–126, doi:10.1061/(ASCE)0733-9429(2002)128:1(117).
- Gregg, M. C., 1999: Uncertainties and limitation in measuring  $\epsilon$  and  $\chi_T$ . *J. Atmos. Oceanic Technol.*, **16**, 1483–1490, doi:10.1175/1520-0426(1999)016<1483:UALIMA>2.0.CO;2.
- Gundersen, J. K., N. B. Ramsing, and R. N. Glud, 1998: Predicting the signal of O<sub>2</sub> microsensors from physical dimensions, temperature, salinity, and O<sub>2</sub> concentration. *Limnol. Oceanogr.*, **43**, 1932–1937.
- Holtappels, M., R. N. Glud, D. Donis, B. Liu, A. Hume, F. Wenzhöfer, and M. M. Kuypers, 2013: Effects of transient bottom water currents and oxygen concentrations on benthic exchange rates as assessed by eddy correlation measurements. *J. Geophys. Res. Oceans*, **118**, 1157–1169, doi:10.1002/jgrc.20112.
- Hume, A. C., P. Berg, and K. J. McGlathery, 2011: Dissolved oxygen fluxes and ecosystem metabolism in an eelgrass (*Zostera marina*) meadow measured with the eddy correlation technique. *Limnol. Oceanogr.*, **56**, 86–96, doi:10.4319/lo.2011.56.1.0086.
- Jonsson, P. R., and Coauthors, 2006: Making water flow: A comparison of the hydrodynamic characteristics of 12 different benthic biological flumes. *Aquat. Ecol.*, **40**, 409–438, doi:10.1007/s10452-006-9049-z.
- Lohrmann, A., R. Cabera, and C. K. Nicholas, 1994: Acoustic-Doppler velocimeter (ADV) for laboratory use. *Fundamentals and Advancements in Hydraulic Measurements and Experimentation*, C. A. Pugh, Ed., ASCE, 351–365.
- Long, M. H., D. Koopmans, P. Berg, S. Rysgaard, R. N. Glud, and D. H. Sogaard, 2012: Oxygen exchange and ice melt measured at the ice-water interface by eddy correlation. *Biogeosciences*, **9**, 1957–1967, doi:10.5194/bg-9-1957-2012.
- , P. Berg, D. de Beer, and J. Ziemann, 2013: In situ coral reef oxygen metabolism: An eddy correlation study. *PLoS One*, **8**, e58581, doi:10.1371/journal.pone.0058581.
- Lorke, A., D. F. McGinnis, and A. Maeck, 2013: Eddy-correlation measurements of benthic fluxes under complex flow conditions: Effects of coordinate transformations and averaging time scales. *Limnol. Oceanogr. Methods*, **11**, 425–437, doi:10.4319/lom.2013.11.425.
- Lorrai, C., D. F. McGinnis, A. Brand, and A. Wüest, 2010: Application of oxygen eddy correlation in aquatic systems. *J. Atmos. Oceanic Technol.*, **27**, 1533–1546, doi:10.1175/2010JTECH0723.1.
- McGinnis, D. F., P. Berg, A. Brand, C. Lorrai, T. J. Edmonds, and A. Wüest, 2008: Measurements of eddy correlation oxygen fluxes in shallow freshwaters: Towards routine applications and analysis. *Geophys. Res. Lett.*, **35**, L04403, doi:10.1029/2007GL032747.
- , S. Cherednichenko, S. Sommer, P. Berg, L. Rovelli, R. Schwarz, R. N. Glud, and P. Linke, 2011: Simple, robust eddy correlation amplifier for aquatic dissolved oxygen and hydrogen sulfide flux measurements. *Limnol. Oceanogr. Methods*, **9**, 340–347, doi:10.4319/lom.2011.9.340.
- Middelburg, J. J., G. Klaver, J. Nieuwenhuize, A. Wielemaker, W. De Haas, T. Vlug, and J. F. W. A. van der Nat, 1996: Organic matter mineralization in intertidal sediments along an estuarine gradient. *Mar. Ecol. Prog. Ser.*, **132**, 157–168, doi:10.3354/meps132157.
- Moncrieff, J. B., R. Clement, J. Finnigan, and T. Meyers, 2004: Averaging, detrending and filtering of eddy covariance time series. *Handbook of Micrometeorology: A Guide for Surface Flux Measurements*, X. Lee, W. J. Massman, and B. E. Law, Eds., Atmospheric and Oceanographic Sciences Library, Vol. 29, Kluwer Academic, 7–31.
- Revsbech, N. P., 1989: An oxygen microsensor with a guard cathode. *Limnol. Oceanogr.*, **34**, 474–478, doi:10.4319/lo.1989.34.2.0474.
- Reynolds, O., 1895: On the dynamical theory of incompressible viscous fluids and the determination of the criterion. *Philos. Trans. Roy. Soc. London*, **186**, 123–164, doi:10.1098/rsta.1895.0004.
- Rheuban, J. E., and P. Berg, 2013: The effects of spatial and temporal variability at the sediment surface on aquatic eddy correlation flux measurements. *Limnol. Oceanogr. Methods*, **11**, 351–359, doi:10.4319/lom.2013.11.351.
- Soetaert K., T. Petzoldt, and F. J. R. Meysman, 2012: Package ‘marelac’: Tools for aquatic sciences, version 2.1.2. R package. [Available online at <http://cran.r-project.org/web/packages/marelac/index.html>.]
- Swinbank, W. C., 1951: The measurement of vertical transfer of heat and water vapor by eddies in the lower atmosphere. *J. Meteor.*, **8**, 135–145, doi:10.1175/1520-0469(1951)008<0135:TMOVTO>2.0.CO;2.